

Articles

Studies of Third-Order Optical Nonlinearities of Model Compounds Containing Benzothiazole, Benzimidazole, and Benzoxazole Units

Mingtang Zhao, Marek Samoc, and Paras N. Prasad*

Photonics Research Laboratory, Department of Chemistry, State University of New York at Buffalo, Buffalo, New York 14214

Bruce A. Reinhardt,* Marilyn R. Unroe, Mark Prazak, and Robert C. Evers

Nonmetallic Materials Division, Air Force Materials Laboratory, Wright-Patterson Air Force Base, Dayton, Ohio 45433-6533

James J. Kane, Chetan Jariwala, and Mark Sinsky

Department of Chemistry, Wright State University, Dayton, Ohio 45435

Received May 8, 1990

To improve our understanding of the molecular structure–nonlinear optical properties relationship, a series of model compounds containing benzothiazole, benzimidazole, and benzoxazole units have been synthesized, and their third-order nonlinear optical properties investigated by using femtosecond degenerate four-wave mixing. For soluble compounds measurements were made with solutions of various concentrations, while for insoluble materials vacuum-evaporated films or melt-quenched films were used. The time–response behavior as well as the concentration dependence of the nonlinearity indicates that there is no one-photon or two-photon resonance encountered at 602 nm, the wavelength of nonlinear optical studies. Therefore, the trend of nonlinearity in the systematically varied model compounds can be related to the structural variations. The present study yields the following information on structure–property relationships: (i) microscopic third-order nonlinearity rapidly increases with an increase of the effective conjugation length for a quasi-one-dimensional molecule; (ii) incorporation of a sulfur-containing heteroaromatic linkage in the conjugated structure enhances the nonlinearity; (iii) transition from a quasi-one-dimensional π -electron delocalization to delocalization in two dimensions introduced by using an imidazole N-linkage enhances the third-order optical nonlinearity without reducing the optical transparency window and at the same time improves the solubility. Possible explanations for these structural effects are presented. Also, the observed qualitative trend is compared with that predicted by a recent semiempirical calculation.

1. Introduction

The search for nonlinear organic materials with very large values of the third-order susceptibility $\chi^{(3)}$ has attracted much interest from the experimental and the theoretical points of view.^{1,2} Until recently most interest has focused on nonlinear materials belonging to the group of π -conjugated polymers. The properties of these polymers still present a challenge to theoreticians and experimentalists because of a variety of new properties brought about by their quasi-one-dimensional structure and the complications due to intermolecular interactions when in the solid state (ordering of chains, interchain charge and energy transfer, local field effects, etc.). However, as is usual in the field of organic materials, at least a part of the necessary knowledge of properties of a solid is gained by studying the properties of molecules building a phase or, which is even more convenient, by studying properties of model molecules resembling sections of a polymer backbone. Our group has undertaken a systematic course of investigations in which model molecules are synthesized

and their third-order hyperpolarizabilities (γ) determined. An integral part of our program is also correlation with theoretical calculations performed using the *ab initio* and semiempirical quantum chemistry methods, which provide feedback necessary for rationalizing the obtained results and acquiring a predictive capability for more complicated systems.³⁻⁷

Our previous studies, as well as those studies by others, have shown how the third-order hyperpolarizability increases as a function of the chain length in oligomers of thiophene,³ benzene,⁴ and pyridine.⁵ It was found that the rapid increase of the γ values as subsequent units are added to the oligomer chain does not persist for long, but a saturation value of γ/N (where N is the number of units in an oligomer chain) is reached. This limiting value is more rapidly attained in the benzene oligomer series than it is in the corresponding thiophene series. This experimental observation is postulated to be due to the more

(1) *Nonlinear Optical and Electroactive Polymers*; Prasad, P. N., Ulrich, D. R., Eds.; Plenum Press: New York, 1988.

(2) *Nonlinear Optical Properties of Polymers*; Heeger, A. J., Orenstein, J., Ulrich, D. R., Eds.; Materials Research Society Symposium Proceedings, Pittsburgh, 1987; Vol. 109.

(3) Zhao, M. T.; Singh, B. P.; Prasad, P. N. *J. Chem. Phys.* **1988**, *89*, 5535.

(4) Zhao, M. T.; Samoc, M.; Singh, B. P.; Prasad, P. N. *J. Phys. Chem.* **1989**, *93*, 7916.

(5) Zhao, M. T.; Perrin, E.; Prasad, P. N., to be published.

(6) Ghosal, S.; Samoc, M.; Prasad, P. N.; Tufariello, J. J. *J. Phys. Chem.* **1990**, *94*, 2847.

(7) Kmínek, I.; Klimovič, Prasad, P. N., to be published.

severe steric interactions of the hydrogen atoms in adjacent benzene rings compared to those same atoms in adjacent thiophenes. Such steric interactions destroy the planarity of the π -conjugated polymer chain and therefore reduce π -orbital overlap. Within our simple coupled oscillator model of oligomeric chains⁸ this corresponds to a lower coupling constant for a system with stronger steric hindrances.

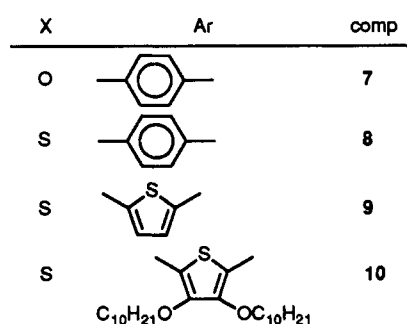
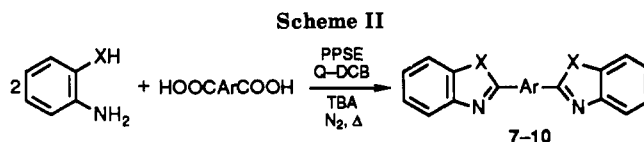
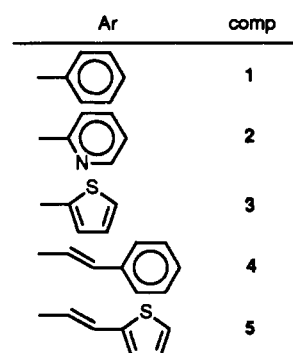
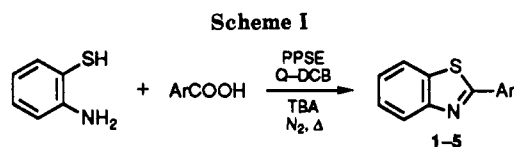
In some cases oligomeric or polymeric molecules made of heterocyclic structures can provide higher γ values not only because of a reduction in steric hindrances but also because of the participation of atomic orbitals of the heteroatoms in the molecular π orbitals. The latter possibility may lead to a higher γ value by virtue of either a stronger overlap between the units or simply by a higher hyperpolarizability of a monomer molecule. In terms of a coupled anharmonic oscillator model considered in ref 8, it means either a higher coupling constant or a larger local anharmonicity of the molecular oscillator.

We present here a study of molecular second-order hyperpolarizabilities for a series of systematically modified molecules whose parent structures are those of benzothiazole, benzoxazole, and benzimidazole. This choice was prompted by the importance of these types of heteroaromatic structures in rodlike polymeric chains that possess interesting mechanical and optical properties. Apart from the concern for the optimization of the structure to obtain the highest values of γ , we are also interested in processability of the obtained materials. Therefore, it is advantageous to build molecules with proper pendant groups that can improve the solubility of oligomers and polymers in organic solvents and/or facilitate processing by spin coating or Langmuir-Blodgett deposition. Obviously modification of molecules by attaching pendant groups also leads to variation of the hyperpolarizability by at least two opposing factors. First, pendant groups may improve the hyperpolarizability by either electron contribution of the pendant to the conjugated π -electron system of the backbone or by induced changes to the electron system by the pendant's inherent polar character. In contrast, the second and opposing factor is the pendant group alteration of the π -electron overlap by steric hindrance.

The syntheses of the molecules investigated in this work have been performed at the Polymer Branch of the Air Force Materials Lab., Wright Research and Development Center, Wright-Patterson Air Force Base, OH, and Wright State University, Dayton, OH. The measurements of the nonlinearities of these molecules were performed by using the degenerate four-wave mixing (DFWM) technique at the Photonics Research Laboratory, State University of New York at Buffalo.

2. Experimental Section

2.1. Syntheses. 2.1.1. Benzoxazole and Benzothiazole Model Compounds. Various preparatory methods were initially considered for the synthesis of both the benzoxazole and benzothiazole model compounds. The standard method of condensation using polyphosphoric acid generally gave lower yields and produced a larger number of byproducts especially with model compounds containing thiophene rings and/or long alkyl ether pendants. It was therefore necessary to develop a new method that could be used as a general method for all the compounds of interest. The method chosen was a modification of a method previously used for simple benzoxazoles⁹ and benzothiazoles.¹⁰ This method involved the direct condensation of aromatic car-



boxylic acids with the appropriate aminophenol, aminothiophenol, or its corresponding hydrochloride salt. The reagent chosen to catalyze the condensation/dehydration was trimethylsilyl polyphosphate (PPSE).¹⁰ In all cases this procedure was found to give moderate-to-high yields of the model compounds while requiring a minimum amount of effort for purification.

The syntheses of benzothiazole model compounds 1-5 were carried out according to Scheme I (procedure A, Appendix). The yields of the model compounds in this series ranged between 60 and 90%.

Bisbenzoxazole and bisbenzothiazole model compounds 7, 8, and 10 were synthesized by the pathway described in Scheme II (procedures B or D, Appendix) in purified yields of 54-83%. The bisbenzothiazole model compound 9 was synthesized in 47% yield by a procedure found in the literature for similar materials¹¹ (procedure C, Appendix).

2.1.2. N-Phenylbenzimidazole Model Compounds. N-Phenylbenzimidazole compound 6 was prepared in moderate yield

(11) Rai, C.; Braunwarth, J. R. *J. Org. Chem.* **1961**, *26*, 3434.

(12) Liechti, P.; Siegrist, A.; Duennenberger, M.; Maeder, E. Ger. Pat. 1,282,021 (Cl. CO6d, D 061), 07 Nov 1968.

(13) Gogte, V. N.; Shah, L. G.; Tilak, L. B. D.; Gaddekar, K. N.; Sahasrabudhe, M. B. *Tetrahedron* **1967**, *23*, 2437.

(14) Gassman, P. G.; Schenk, W. N. *J. Org. Chem.* **1977**, *42*, 918.

(15) Lazarus, S. D.; Twilley, I. C. Fr. Patent 1,462,569 (Cl. C 08g), 16 Dec 1966; CA 67: P64886j.

(16) Osuka, A.; Uno, Y.; Horiuchi, H.; Suzuki, H. *Synthesis* **1984**, *2*, 145.

(17) Addison, A.; Nageswara Rao, T.; Wahlgren, C. G. *J. Heterocycl. Chem.* **1983**, *20*, 1481.

(18) Cohen, V. *J. Heterocycl. Chem.* **1979**, *16*, 13.

(19) Kaupp, G.; Grundken, E.; Matthies, D. *Chem. Ber.* **1986**, *119*, 3109.

(20) Reid, W.; Hinsching, S. *Liebigs Ann. Chem.* **1956**, *608*, 47.

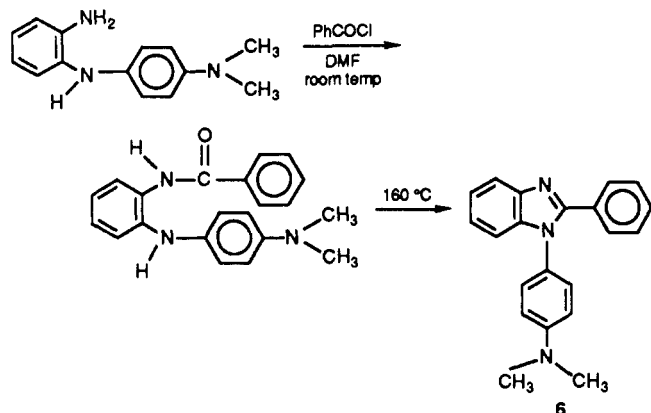
(21) Moyer, W. *J. Polym. Sci.* **1965**, *A3*, 2107.

(8) Prasad, P. N.; Perrin, E.; Samoc, M. *J. Chem. Phys.* **1989**, *91*, 2360.

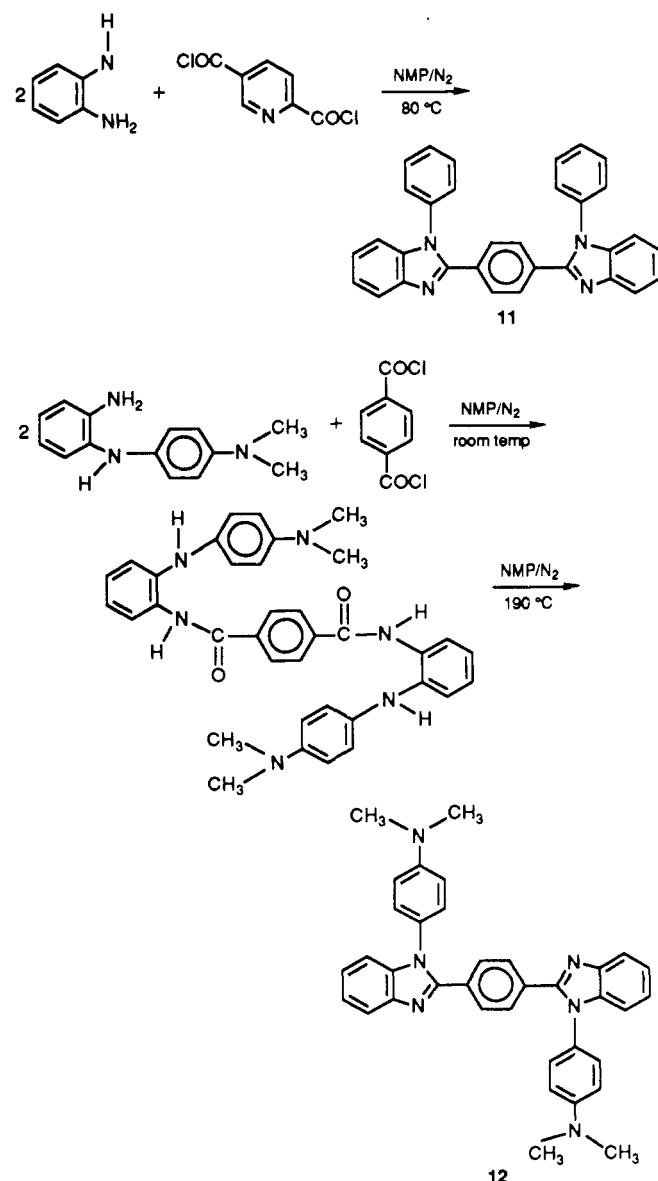
(9) Aizpurua, J. M.; Palomo, C. *Bull. Soc. Chim. Fr.* **1984**, *3-4*, 142.

(10) Yamamoto, K.; Watanabe, H. *Bull. Chem. Soc. Jpn.* **1982**, *1225*.

from the thermal ring closure of neat *N*-(4-(dimethylamino)-phenyl)-*N'*-benzoyl-1,2-phenylenediamine (procedure E, Appendix).



N-Phenyl-substituted bisbenzimidazoles 11 and 12 were prepared in fair to good yields by the ring closure in aprotic solution of either the in situ generated bisamide (procedure F, Appendix) or the isolated terephthalamide (procedure G, Appendix).



2.2. Measurements of Third-Order Hyperpolarizabilities.

Degenerate four-wave mixing is a phenomenon in which the presence of three optical fields of the same frequency ω produces

a nonlinear polarization at the same frequency that becomes the source of the fourth beam. The direction of this beam is given by the phase-matching condition, i.e., the condition of conservation of the wave vector \mathbf{k} . An equivalent description of the DFWM phenomenon is in terms of transient gratings formed by interaction of pairs of beams and the Bragg diffraction of the remaining beam from the phase and/or amplitude grating.²²⁻²⁴

Degenerate four-wave mixing measurements were performed in a backward beam geometry (cf. ref 3) or in a BOXCARS geometry (forward four-wave mixing). The laser system was the same as described in previous publications.³ It delivered amplified nearly transform limited 400-fs pulses at 602 nm with the repetition frequency of 30 Hz and maximum energy of approximately 0.4 mJ/pulse. An appropriate set of beam splitters was used to form three beams that could be synchronized with delay lines to arrive at the sample at the same time. The delay of one of the beams (the backward beam in the backward beam geometry or the out-of-plane beam in the BOXCARS geometry) could then be varied to record the temporal profile of the DFWM signal. The signal could be observed as the phase conjugate to one of the forward beams in the backward beam geometry and in the position given by the appropriate phase-matching condition in the BOXCARS case. The signal was monitored with a photodiode and processed with a boxcar average (EG&G Princeton Applied Research, Model 4200).

The intensity of the DFWM signal for liquid or solid samples corresponding to the maximum of the profiles obtained by scanning the delay was compared to the signal obtained for a reference sample under the same light-intensity conditions. The bulk third-order susceptibility of the sample was then calculated from this comparison by using

$$\chi^{(3)} = (I/I_s)^{1/2} (n/n_s)^2 (L_s/L) \chi_s^{(3)} \mathcal{F} \quad (1)$$

where I stands for the DFWM signal intensity, n is the refractive index of the medium, L is the interaction length, the subscript s refers to a reference sample, and \mathcal{F} is the correcting factor taking into account the sample absorption. For those measurements performed on materials in the form of solid films, the obtained $\chi^{(3)}$ refers in a straightforward way to the microscopic hyperpolarizability of the investigated molecules. For measurements in solutions, however, the contribution of the solvent nonlinearity must be taken into account. Therefore, the macroscopic third-order susceptibility is then taken as

$$\chi^{(3)} = f^4 (N_s \gamma_s + N_x \gamma_x) \quad (2)$$

where γ_s and γ_x stand for the hyperpolarizabilities of the solvent and the solute, respectively, N_s and N_x denote the respective number densities of molecules, and f is the local field factor approximated in this paper by the Lorentz expression, i.e.

$$f = (n^2 + 2)/3 \quad (3)$$

where n is the refractive index of a solution at the frequency of the measurements (i.e., at 602 nm). These values were approximated by using Abbe refractometer measurements at the sodium line (589 nm). Equation 2 was used to obtain least-squares fitted values of γ_s and γ_x for each series of concentration dependences of $\chi^{(3)}$. Errors in the determination of γ were calculated taking into account the uncertainties of the measurements of the DFWM intensities for individual points. The uncertainties of the DFWM intensities for individual points. The uncertainties of the γ values depended on experimental factors such as the concentration range used for the measurements, the number of data points, and the ratio of the solute and solvent hyperpolarizabilities. Additional errors could have been introduced by the inaccuracy of our approximation of local field factors, which in some cases utilized refractive index calculated from the additivity of molecular linear polarizabilities. Since in most cases we used dilute solutions for

(22) Shen, Y. R. *The Principle of Nonlinear Optics*; Wiley Interscience: New York, 1984.

(23) *Optical Phase Conjugation*; Fisher, R. A. Ed.; Academic Press: New York, 1983.

(24) Eichler, H. J.; Günter, P.; Pohl, D. W. *Laser-Induced Dynamic Gratings*; Springer-Verlag: Berlin, 1986.

Table I. Properties of Benzoxazole and Benzothiazole Model Compounds

compd	synth proc	mp (solvt), °C; yield, %	lit mp (solvt), °C; lit ref	elem anal (calcd, found) or CARN ^a	IR spectra ν , cm ⁻¹
1	A	115.5–116.5 (ethanol); 90	115–116 (ethanol); 16	883-93-2	1480, 1440, 1320, 11230, 1075, 965, 770, 735, 690
2	A	135–136 (MeOH/H ₂ O); 73	133–135 (ethanol); 17	716-80-3	1583, 1456, 1316, 982, 978, 727
3	A	101–103 (MeOH/H ₂ O); 78	98–100 (EtOH/H ₂ O); 18	34243-38-4	1545, 1420, 1920, 760, 710, 700
4	A	112–114 (hexane); 81	115 (ethanol); 19	104505-71-7	1628, 1500, 1480
5	A	118–119 (hexane); 60	117 (EtOH/H ₂ O); 20	5132-04-7	1622, 14850, 1175, 950, 760, 690
6	E	256–257 (DMF/acetone); 66		C 80.48, 80.67; H 6.118 6.05; N 13.41, 13.38	2895, 1608, 1525, 1474
7	B	356–357 (xylene); 85	355–356 (pyridine); 21	904-39-2	1548, 1452, 1413, 1245, 1059, 850, 760, 745
8	B	263–265 (xylene); 83	257–258 (benzene); 11	5153-65-1	1480, 1433, 1312, 965, 763
9	C	241–242 (toluene); 47	232–233 (DMF); 12	18013-43-9	1547, 1507, 1462, 1430, 1263, 920, 756, 697
10	D	92–93 (abs ethanol); 54		C 68.83, 68.93; H 7.60, 7.36; N 4.23, 4.00	2925, 2850, 1515, 1320, 1050, 755, 725
11	F	238–240 (EtOH/H ₂ O); 45		C 80.33, 80.52; H 4.57, 4.69; N 15.11, 15.06	3054, 1595, 1499
12	G	>320; 73		C 78.81, 79.15; H 5.88, 5.80; N 15.32, 15.30	2889, 1606, 1526, 1454

^aChemical Abstracts Service registry number.

which the refractive index was only slightly different from that of the solvent, these errors should, however, be very small. In contrast, larger errors may be encountered for measurements on solid films, where usually only a rough estimate of the refractive index could be made due to the nonuniformity of the films. We estimate that our values of γ obtained from measurements on solid films bear a total error limit of about 20%.

The hyperpolarizabilities entering eq 2 are orientational averages of the respective fourth-rank tensors of γ_{ijkl} . In the case of measurements on solid films of neat substances, eq 2 simplifies because there is no solvent contribution; however, there may be other complications due to imperfect orientational averaging in thin films and, possibly, inadequacy of the assumption of the isotropic Lorentz local field factor. For lack of better knowledge, we calculated, however, the average γ values for thin films using an approximation of an isotropic medium.

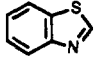
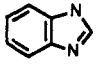
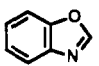
2.3. Preparation of Thin Films. For those compounds that were not sufficiently soluble in tetrahydrofuran, the DFWM measurements were performed on thin solid films. Two methods of preparation were utilized: vacuum deposition and quenching of the melt. The vacuum deposition was performed at deposition rates between 30 and 50 Å/s in a vacuum chamber where the vacuum was kept at 10^{-6} – 10^{-5} Torr. Microscope glass slides were used as substrates. The deposition rate and the final thickness of the film were estimated by using a quartz crystal film-thickness monitor (FTM4). In some cases the thickness was also calibrated by dissolving the film from a given area in a known volume of a solvent and determining the concentration by using UV-visible absorption spectra of the solution. Alternatively, the thicknesses were measured with a profilometer (Model α -4).

The vacuum evaporation usually gave acceptable optical-quality films only for those materials that contained relatively large molecules. For low molecular weight substances the obtained films exhibited microcrystalline structure and excessive light scattering that prohibited any optical measurements. In those cases we resorted to preparation of thin films by fast quenching of the compounds melted under nitrogen on microscope glass slides. This procedure often gave films with reasonably good quality areas of a few square millimeters, which were then used for the measurements. Areas of the film that gave the lowest scattering were selected. The nonuniformity of the films, unknown orientation of the crystals, and a relatively large error in the determination of the film thickness all contribute to a large uncertainty in the results for γ obtained on this type of samples.

3. Results

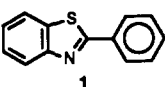
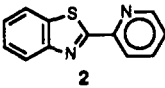
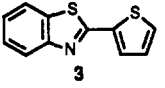
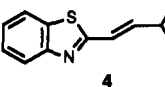
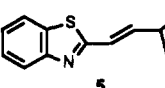
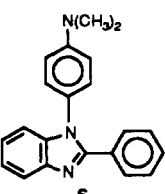
The values of γ obtained from DFWM measurements for all molecules investigated in this study are listed in Tables II–IV. Additionally, we also list positions of UV-vis absorption maxima for solutions of these molecules. According to structural similarity, we divided the inves-

Table II. Maximum UV-Vis Absorption Peaks, λ_{\max} , and Second-Order Hyperpolarizability Values, γ , for Benzothiazole, Benzoxazole, and Benzimidazole

compd	λ_{\max} , ^a nm	γ , esu
	294.5 (2) 284.1 (2) 250.8 (1)	$2.6 \times 10^{-35} \pm 3.4 \times 10^{-36}$
	281.1 (2) 274.3 (2) 245.6 (1)	$2.0 \times 10^{-35} \pm 3.0 \times 10^{-36}$
	277.0 (2) 270.7 (2) 239.0 (1)	$1.6 \times 10^{-35} \pm 3.2 \times 10^{-36}$

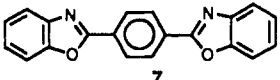
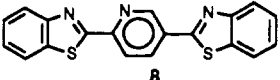
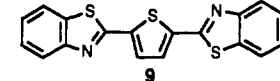
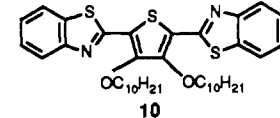
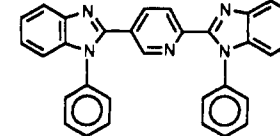
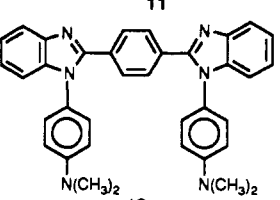
^aThe number in the parentheses refers to the relative intensities of the absorption peaks.

Table III. Maximum UV-Vis Absorption Peaks, λ_{\max} , and Second-Order Hyperpolarizability Values, γ , for Molecules with Two Connecting Aromatic Units

	method	λ_{\max} , ^a nm	γ , esu
	THF	297.2	$4.3 \times 10^{-35} \pm 5.7 \times 10^{-36}$
	THF	309.4	$4.7 \times 10^{-35} \pm 4.8 \times 10^{-36}$
	THF	325.8	$5.4 \times 10^{-35} \pm 1.1 \times 10^{-35}$
	THF	337.7	$7.7 \times 10^{-35} \pm 1.8 \times 10^{-35}$
	THF	355.8	$8.8 \times 10^{-35} \pm 1.5 \times 10^{-35}$
	THF	295.8 (2) 267.8 (1)	$1.1 \times 10^{-34} \pm 3.4 \times 10^{-35}$

^aThe number in the parentheses refers to the relative intensities of the absorption peaks.

Table IV. Maximum UV-Vis Absorption Peaks, λ_{\max} , and Second-Order Hyperpolarizability Values, γ , for Molecules with Three or More Connecting Aromatic Units

compd	method	λ_{\max} , ^a nm	γ , esu
 7	film	357.6 (3) 339.5 (1) 325.0 (2)	9.0×10^{-35}
 8	film	367.0 (3) 352.0 (1) 337.0 (2)	1.9×10^{-34}
 9	THF	397.0 (3) 385.8 (1) 368.2 (2)	$2.6 \times 10^{-34} \pm 1.2 \times 10^{-34}$
 10	THF	412.6 (3) 390.2 (1) 371.0 (2)	$3.9 \times 10^{-34} \pm 2.8 \times 10^{-35}$
 11	THF	339.6	$1.1 \times 10^{-33} \pm 2.4 \times 10^{-34}$
 12	film	325.2 (2) 268.0 (1)	2.2×10^{-33}

^a The number in the parentheses refers to the relative intensities of the absorption peaks.

tigated molecules into various groups to facilitate comparisons and explanations.

In the process of discussing the dependence of the γ values on the structure of molecules we use simple qualitative concepts. The molecules investigated by us can be roughly considered as one-dimensional systems. In such systems one expects the dominant contribution to the orientationally averaged γ to be that along the molecule backbone (z axis), i.e., γ_{zzzz} . In a simple picture given by Rustagi et al., the $\chi^{(3)}_{zzzz}$ is given as follows:

$$\chi^{(3)}_{zzzz} \propto \frac{e^{10}}{\sigma} \left(\frac{a_0}{d} \right)^3 \frac{1}{E_g^6} \quad (4)$$

where a_0 is the Bohr's radius, d is the average distance between neighboring carbon atoms, σ is the cross-sectional area per chain, and E_g is the energy gap of the molecule. As a result, a molecule having a smaller bandgap will have a larger $\chi^{(3)}$ and γ . The bandgap, in turn, should depend on the degree to which the π -electrons are delocalized along the molecular backbone. In a simple one-dimensional picture one often can talk about an effective "conjugation length". Obviously, the larger the conjugation length, the smaller the bandgap and the larger the hyperpolarizability. In the following we discuss the nonlinearity of specific molecules as well as the changes in their absorption spectra with the increasing chain length.

3.1. Benzothiazole, Benzimidazole, and Benzoxazole. The three heterocyclic molecules were studied in THF solutions. The concentration ranges were as follows: (i) benzothiazole, 0.25–4.0 M; (ii) benzimidazole, 0.2–0.8 M; (iii) benzoxazole, 0.5–3.0 M. For each molecule, several THF solutions with different concentrations are studied, and the corresponding DFWM signals are obtained. As an example, Figure 1 shows the temporal be-

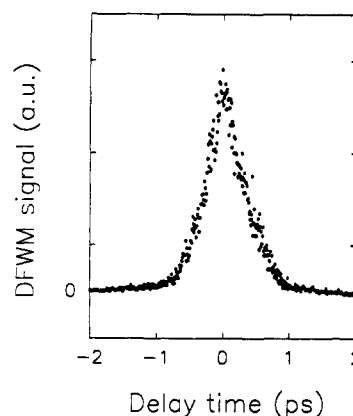


Figure 1. Time-resolved degenerate four-wave mixing (DFWM) signal for a 0.5 M solution of benzoxazole in tetrahydrofuran (THF).

havior of the DFWM signal for a benzoxazole solution. The symmetric curve indicates that there is no one-photon or two-photon absorption involved in the degenerate four-wave mixing process for this molecule at the measured wavelength of 602 nm. The presence of any population grating induced by one-photon or two-photon absorption will result in an asymmetrically temporal DFWM signal. For the other two molecules, as well as the molecules which will be discussed in the following two subsections, the temporal studies of DFWM signal do not show any asymmetry either. It is therefore confirmed that the γ values for the three molecules at 602 nm are nonresonant values. This inference is also supported by the concentration-dependence study of $\chi^{(3)}$, which yields a positive real value of γ for each compound. In the case of a one-photon or two-photon resonance, the γ value is not necessarily pos-

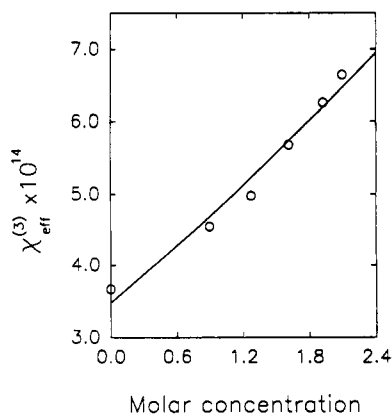


Figure 2. Concentration dependence of effective $\chi^{(3)}$ of benzoxazole solutions in THF. The hollow circles are the data points and the solid curve is the fit by using eq 2.

itive and it is always a complex quantity. Figure 2 shows the concentration dependence of effective $\chi^{(3)}$ for the benzoxazole molecule whose γ value can be obtained by fitting the concentration dependence. The γ values for other two molecules can be obtained in the same way and are summarized in Table II. Also listed are the positions of dominant absorption peaks, obtained from measurements in THF solutions. The letters in parentheses refer to the intensities of the peaks. Generally, these absorption transitions are either of $n\pi^*$ or $\pi\pi^*$ type, the $n\pi^*$ transitions corresponding to lower energies but smaller oscillator strengths. On the basis of the description of molecular hyperpolarizabilities in terms of the sum-over-states approach, one would expect that there will be a larger contribution to γ from the $\pi\pi^*$ transitions than from the lower lying $n\pi^*$ transitions. However, the relative importance of those two types of transitions cannot be assessed with any confidence without the knowledge of all the terms entering the sum-over-states expression.

The γ values in Table II show that the nonlinearity decreases in the order benzothiazole, benzimidazole, and benzoxazole. This is also what would be expected from the shifts in the positions of the corresponding absorption peaks. Qualitatively, this ordering of the absorption transitions and the nonlinearity for the three molecules can be explained as follows. The heteroatoms donate p-electrons to the molecular π orbitals of the heteroaromatic molecules. However, while the electronegativity of the sulfur atom is not very different from that of a carbon atom, the electronegativity of nitrogen is markedly larger, and that of oxygen is the largest in the considered series. Therefore, the distribution of the electronic density will be more equally shared between sulfur and carbon than between nitrogen or oxygen and carbon. Consequently, the π orbitals in sulfur-containing heteroaromatics are better delocalized than in molecules containing nitrogen or oxygen. In the case of sulfur an important factor may also be the presence of empty d orbitals that can contribute to the molecule π orbitals. The net effect of this contribution will also be a reduction in the energy of the $\pi\pi^*$ transition, and, consequently, a higher hyperpolarizability.

3.2. Molecules with Two Aromatic Units. Since benzothiazole has the highest γ value among the three molecules considered above, it seemed worthwhile to investigate the nonlinearity of more extended π -electron systems containing benzothiazole. The first three molecules listed in Table III involve linkage of benzothiazole with benzene, pyridine, and thiophene. In all three cases, the hyperpolarizability is strongly enhanced in comparison

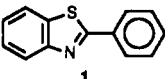
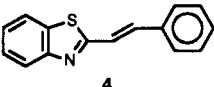
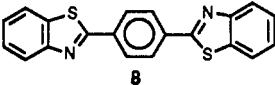
to the benzothiazole unit, which is not an unexpected result. The second-order hyperpolarizability increases very fast with the extension of the π -electron system and is certainly far from being additive when additional aromatic units are attached. The observed differences between the three molecules are only slight, but it is worth noticing that the highest hyperpolarizability and the smallest bandgap are observed for the thiophene derivative of benzothiazole. The explanation for this difference is not obvious. One factor here may be the different degree of overlap of π -electron systems of benzothiazole with its partner in the three systems. Deviations from planarity in these molecules will modify this overlap. An additional contribution may come from the presence of lone electron pairs on nitrogen in the case of pyridine unit and sulfur in the case of thiophene unit.

Molecules 4 and 5 involve the linkage of benzothiazole with benzene and thiophene through an ethylene bridge. Again, the enhanced π -electron conjugation is manifested by the increased values of γ and the decreased bandgap. Obviously, these two effects can be expected to appear together and, in consequence, lead to limitations on the feasibility of building highly nonlinear molecules with a reasonable optical-transparency range. In this light a very interesting result is that obtained for molecule 6. Although a less nonlinear unit of benzimidazole is used here instead of benzothiazole, the nonlinearity of this molecule is much higher than that of molecule 1. It should be noted that the transparency ranges of these two molecules are approximately the same. One should conclude that the enhancement of γ is due to the presence of the side group attached to the benzene ring of benzimidazole. One obvious reason for this enhancement is that molecule 6 is, unlike the other molecules considered here, a two-dimensional π -electron system. Therefore, the orientationally averaged γ value should contain relatively high additional contributions, apart from γ_{zzzz} , that is, for example, γ_{xxxx} and γ_{zzxz} , if xz is taken as the molecular plane. The introduction of the $(CH_3)_2N$ group, a strong electron donor, may also have a beneficial effect on the nonlinearity, as its presence will modify the electron distribution in the molecule, possibly leading to a higher anharmonicity of the potential acting on π electrons. An added benefit of introducing such groups is also an improvement in the solubility of the molecule, which is important for the processing of any nonlinear optical material built by using such molecular units.

3.3. More Complicated Combinations of Heterocyclic Molecules. We discuss here the nonlinear optical properties of more complicated heteroaromatic molecules whose structures are given in Table IV. Because of the larger number of π electrons that can take part in the conjugation or because of an increased conjugation length, the γ values of these molecules are markedly higher than the values for smaller π -electron systems considered in the previous subsection. The trend of hyperpolarizability changes observed for this series of molecules is again intuitively predictable. Molecule 8 exhibits a higher hyperpolarizability than that of 7. This is also accompanied by a lowering of the energy of the electronic transitions in 8. As both molecules have approximately the same length, this difference comes from the differences of properties of respective parent molecules, i.e., benzothiazole and benzoxazole. Qualitatively, one can attribute the differences to a better conjugation in the benzothiazole derivative.

A comparison between 8 and 9 must be taken with some caution because one of the compounds was investigated

Table V. Experimentally Determined and Theoretically Calculated Second-Order Hyperpolarizabilities, γ , for Some Representative Benzothiazole Model Compounds

compd	exptl γ , esu	theoret	
		conformation	γ (esu)
 1	4.3×10^{-35}	staggered planar	6.2×10^{-35} 2.41×10^{-34}
 4	7.7×10^{-35}	trans-staggered trans-planar	2.19×10^{-34} 6.14×10^{-34}
 8	1.9×10^{-34}	planar	1.227×10^{-33}

in the form of a solid film while the other in THF solutions. As already discussed, this can lead to some differences due to, e.g., an inadequacy of the assumption of orientational averaging for γ in the solid as well as a shift in the position of the electronic resonances. However, it is comforting to find that the difference between γ for 8 and 9 is at least qualitatively in agreement with our expectations, namely, the compound in which bridging of the two benzothiazole units involves thiophene has a higher γ value. By substituting two thiophene hydrogens with alkoxy groups, one obtains molecule 10, which, apart from having a greater γ value than 9, is also characterized by a better solubility in organic solvents.

Finally, molecules 11 and 12 are not truly one-dimensional systems, and both show greatly increased γ values. It is very interesting to find that this increase of nonlinearity is not accomplished at the expense of reduced transmittance window, i.e., a decrease in the bandgap. Obviously, the qualitative rule for one-dimensional systems relating an increase in γ to the decrease in the bandgap as the conjugation is enhanced (by adding more π -electron units to the chain or improving their overlap) does not hold for two-dimensional systems. The larger γ value for molecule 12 than that for molecule 11 is believed to be derived from the very strong electron donor groups $N(C_6H_5)_2$, the participation of which usually enhances the γ value for structures such as molecule 6. Therefore, this type of approach of adding pendant groups capable of introducing two-dimensional π -electron delocalization appears to be highly promising for enhancing the nonresonant third-order optical nonlinearity and at the same time improving the solubility for materials processing.

4. Discussion

We have shown that the third-order optical nonlinearities of organic molecules can be substantially improved if a judicious procedure of building a molecule from optimized units is performed. Generally, the third-order nonlinear optical properties of such systematically constructed molecules have been interpreted in a qualitative way just by considering changes in the delocalization of π electrons as additional units are added to a molecule or it is modified by substitution of carbon atoms with heteroatoms. Theoretical calculations on some of the listed compounds have been performed by Goldfarb et al.²⁵ using a semiempirical method involving MNDO approximation with the finite-field (FF) approach. Since this method utilizes a static field, the calculated γ values are molecular static hyperpolarizabilities that represent either the ex-

trapolation to low frequency or a nonresonant case. For comparison, these calculated γ values as well as the experimental γ values are listed in Table V, in which the structural conformation assumed for the theoretical calculation is specified. Although this approach does not in general produce a quantitatively reliable computation of γ , a qualitative trend for a systematically varied structure can be deduced.

By comparing the theoretically computed values with the experimental results, a general conclusion is that the experimentally determined γ values for these molecules are more or less smaller than the theoretically calculated ones for respective molecules and the discrepancy increases with the molecule size. Besides the experimental errors in the measurement of γ values, the limitation of the approximation for the theoretical model may play an even more significant role in causing such γ discrepancy. However, both experimentally determined and theoretically calculated γ values show the same increasing trend as the molecules become larger.

There are several issues to be addressed before attempting to derive any conclusion from a systematic study such as the one described in this paper. The first important issue is the reliability of the data obtained by us and the comparisons made between results obtained for various molecules. We have already stated that meaningful comparisons can only be made between orientationally averaged values of the hyperpolarizabilities. Obviously, solution measurements are, therefore, superior to measurements performed on solid samples. However, in both cases, we attempt to compare molecular properties derived from measurements of a macroscopic quantity $\chi^{(3)}$. Although the use of the simple Lorentz approximation for the local field factor is widespread, there is actually no sound justification for the use of this approximation. One can expect that the approximation of an isotropic local field factor may break down in case of an anisotropic solid, especially that containing very asymmetric molecules (e.g., quasi-one-dimensional oligomers or polymers). The reliability of any hyperpolarizability data derived from solution measurements would appear to be better. However, in the case of degenerate four-wave mixing, one deals with a process described formally by a third-order susceptibility, $\chi^{(3)}(-\omega; \omega, -\omega, \omega)$, i.e., all interacting fields have the same frequency. The third-order nonlinear interaction can sometimes be viewed as a change in the susceptibility induced by interaction of two fields and generation of a nonlinear polarization by probing with a third field. In the degenerate case all fields have the same frequency. Therefore, an interaction of two fields leads to a change in susceptibility that does not oscillate in time. The third field of frequency ω generates a nonlinear polarization at the same frequency. However, the appearance of a time-

(25) Goldfarb, J.; Medrano, J. *Nonlinear Optical Effects in Organic Polymers*; Messier, J., Kajzar, F., Prasad, P., Ulrich, D., Eds.; Kluwer Academic Publishers: Dordrecht, 1989; p 93.

independent term in the interaction of two optical fields leads to the inclusion of all low-frequency material modes in the nonlinear process producing the susceptibility change. In practice, the duration of laser pulses is the limitation for the frequencies involved. Nevertheless, even with picosecond or subpicosecond pulses one always can expect that molecular motions having the characteristic frequencies of the order of 10^{-12} s can give a contribution to the observed nonlinearity. In the case of liquids, the dominant process, apart from the electronic nonlinearity, is the reorientation of anisotropic molecules in the optical field. Such reorientation depends on the anisotropy of the molecular polarizability tensor α_{ij} ; its characteristic time constants can be in picoseconds or even femtoseconds. In the case of solids the molecular motions are limited to small amplitude vibrations and translations, but their contribution should also be present.

These uncertainties concerning the role of γ anisotropy and the contributions of reorientational (nuclear) nonlinear hyperpolarizability make the comparisons between results for various molecules rather difficult. An additional factor is that of dispersion of γ . While from the technological point of view the relevant value is the susceptibility at the combination of frequencies to be used in an application, a comparison between properties of various molecules would be more meaningful if the electronic hyperpolarizability could be extrapolated to zero frequency. Otherwise, an enhancement of the hyperpolarizability due to, for example, substituting a nitrogen in a heterocyclic molecule with a sulfur can be interpreted as a dispersion effect, i.e., the result of the shift of electronic resonances to lower energies. In our case an attempt to extrapolate our experimental results to zero frequency to obtain "static" hyperpolarizabilities may not be useful because of the uncertainty regarding the contributions of various excited states to the total hyperpolarizability. As already mentioned, the presence of both $n\pi^*$ and $\pi\pi^*$ excitations leads to a dispersion relation for γ that must include both types of excited states as well as transitions between them. Therefore, at the present time we are limited to a comparison between the data taken at a single frequency.

Our qualitative comparisons lead, therefore, to the following conclusions:

(i) Molecular hyperpolarizabilities in quasi-one-dimensional molecules increase very rapidly with the length of the conjugated π -electron system.

(ii) Inclusion of heteroatoms in the π -electron system can be beneficial for the nonlinearity, due to either the role of additional p and/or d orbitals provided by the heteroatoms or the role of steric factors in the π -electron conjugation.

(iii) Sulfur-containing aromatic links are more nonlinear than those containing nitrogen and/or oxygen.

(iv) A transition from one-dimensional π -electron conjugation to two-dimensional systems using imidazole N-linkage can enhance third-order optical nonlinearity without reducing the bandgap and at the same time improve the solubility.

Acknowledgment. The work performed at SUNY, Buffalo, was supported by the Air Force Office of Scientific Research, Directorate of Chemical and Atmospheric Sciences and Polymer Branch, Air Force Wright Materials Laboratory, Wright Research and Development Center through Contract Number F49620-90-C-0021.

Appendix

All solvents, commercially available, were distilled and stored over molecular sieves (Linde 4A) before use. All other reagents

were used without further purification. Thin-layer chromatography (TLC) was performed either on precoated plastic silica gel strips with UV-254 indicator (Beckmann Instruments, Inc., Westbury, NY) or on glass-precoated KC18 reverse-phase plates with UV-254 indicator (Whatman, Ltd.). Melting points were uncorrected. Electron impact mass spectra (EIMS) were performed on a Finnegan Model 4021 GC/MS/DS system. Infrared spectra were recorded on a Beckmann IR-33 using KBr films; values were reported in wavenumbers (cm^{-1}). Physical properties, elemental analyses, literature references, and infrared spectral data for all model compounds are summarized in Table I.

For *N*-phenylbenzimidazoles and their precursors, infrared (IR) spectra were recorded on a Nicolet 5DX spectrometer. Elemental analyses were done at Midwest Microlab, Indianapolis, IN, and at the Department of Chemistry, Wright State University. Proton NMR spectra were carried out on a Varian EM 360A NMR, and ^{13}C NMR spectra on a Bruker AC100 (internal standard TMS). Mass spectrometric analyses were done on Finnigan MAT (INCOS 50) and Finnigan 4021 mass spectrometers.

Procedure A. A mixture of *o*-aminothiophenol (0.005 mol), the appropriate aromatic carboxylic acid (0.005 mol), PPSE (6.0 g), and *o*-dichlorobenzene (15 mL) was stirred at room temperature under nitrogen while tri-*n*-butylamine (TBA) (0.01 mol) was added dropwise. After the addition of base was completed, the reaction mixture was heated at 85 °C under nitrogen for 18 h. The temperature was then raised to 135 °C for 18 h and finally to 165 °C for 4 h. At the end of the final heating period the reaction mixture was allowed to cool to room temperature and poured into water (200 mL). This mixture was then extracted twice with methylene chloride (100 mL each) and separated. The combined methylene chloride extracts were washed with water (200 mL) and dried over anhydrous magnesium sulfate. The solvent was removed under reduced pressure, and the resulting oily solid was stirred with methanol (50 mL). The resulting solid was then purified by recrystallization from the appropriate solvent (Table I).

Procedure B. A mixture of the appropriate aromatic dicarboxylic acid (0.005 mol), either *o*-aminophenol or *o*-aminothiophenol (0.01 mol), PPSE (12.0 g), and *o*-dichlorobenzene (30 mL) was stirred at room temperature under nitrogen. To this mixture TBA (0.02 mol) was added dropwise, and the temperature was raised to 85 °C for 18 h. The temperature was then raised to 135 °C for 18 h and finally to 165 °C for 4 h. The reaction mixture was allowed to cool to room temperature and poured into methanol (500 mL). The resulting solid was filtered, air dried, and recrystallized from appropriate solvent (Table I).

Procedure C. 2,5-Bis(benzothiazol-2-yl)thiophene (9). A mixture of 2,5-thiophenedicarboxylic acid (1.01 g, 0.006 mol) and *o*-aminothiophenol (1.52 g, 0.012 mol) in polyphosphoric acid (15 g) was stirred and heated under nitrogen at 140 °C for 2 h. The temperature of the reaction mixture was then raised to 155 °C for 15 h. The dark red solution was allowed to cool to approximately 60 °C and poured into water (150 mL). The resulting mixture was neutralized to pH 8 with ammonium hydroxide. The solid was filtered, washed with water, and air dried to give a crude yellow product (1.85 g, 90%). Three recrystallizations from toluene afforded compound 9 (1.08 g, 47%), mp 241–242 °C. This compound had a melting point that differed from the literature value¹² but gave satisfactory elemental and mass spectral analyses (Table I).

Procedure D. 2,5-Diethyl 3,4-Bis(decyloxy)thiophene Dicarboxylate. A mixture of 2,5-diethyl 3,4-dihydroxythiophenedicarboxylate¹³ (52.1 g, 0.20 mol), 1-bromodecane (93.38 g, 0.42 mol), and potassium carbonate (30.04 g, 0.22 mol) in *N,N*-dimethylformamide (300 mL) was heated at 100 °C under nitrogen for 20 h. The reaction mixture was allowed to cool to room temperature, and the suspended potassium bromide salts were filtered from the solution over diatomaceous earth. The filtrate was divided into two portions and poured into water (2500 mL each). The crude product was solidified after the aqueous solution was stirred for 30 min. The solid was filtered, air dried, and recrystallized from methanol (5000 mL). The product was dried at room temperature under reduced pressure to afford colorless plates (80.65 g, 75%), mp 39–40 °C. Anal. Calcd for $\text{C}_{30}\text{H}_{50}\text{O}_6\text{S}$: C, 66.88; H, 9.73; S, 5.95. Found: C, 66.57; H, 9.39; S, 5.96. FTIR (KBr) ν (cm^{-1}) 2920, 1725, 1550, 1490, 1285, 775; EIMS (70 eV) m/z 540 (M^+ , 1), 204 (100).

3,4-Bis(decyloxy)-2,5-thiophenedicarboxylic Acid. In a modification of a reported procedure¹⁴ a suspension of 2,5-diethyl 3,4-bis(decyloxy)thiophenedicarboxylate (50.0 g, 0.93 mol) in tetrahydrofuran (THF, 1500 mL) was slowly added to a cold (0–5 °C), rapidly stirring slurry of potassium *tert*-butoxide (62.5 g, 0.57 mol) and water (7.5 mL). The solution was allowed to warm to room temperature over 24 h. TLC on both a reverse-phase plate (80:20 ethanol:water) and silica gel strip (9:9:1 diethyl ether:hexane:acetic acid) indicated the absence of starting material. The potassium salts were filtered from the solution and washed with THF (250 mL) until TLC indicated the absence of trapped product. The solution was then reduced in volume to approximately 300 mL and poured into water (1500 mL). The crude diacid was precipitated after acidification with 37% hydrochloric acid (125 mL). The product was recrystallized first from toluene (800 mL) and finally from methanol (800 mL) to afford a white powder (44.28 g, 94%), mp 182–183 °C. Anal. Calcd for C₂₆H₄₄O₆S: C, 64.44; H, 9.15; S, 6.62. Found: C, 64.36; H, 8.61; S, 6.55. FTIR (KBr) ν (cm⁻¹) 2920, 1680, 1655, 1298, 1200, 940, 775; EIMS (70 eV) m/z 484 (M⁺, 0.44), 204 (100).

3,4-Bis(decyloxy)-2,5-bis(benzothiazol-2-yl)thiophene (10). To a mixture of 3,4-bis(decyloxy)-2,5-thiophenedicarboxylic acid (2.42 g, 0.005 mol), *o*-aminothiophenol (1.37 g, 0.01 mol), and PPSE (12.0 g) in *o*-dichlorobenzene (30 mL) under nitrogen was dropwise added TBA (7.42 g, 0.04 mol) over 20 min. The reaction mixture was slowly heated to 85 °C for 18 h. The temperature of the reaction mixture was then raised to 135 °C over 6 h and maintained at that temperature for an additional 18 h. The reaction mixture was allowed to cool to room temperature, and the *o*-dichlorobenzene was removed under reduced pressure. The resulting solid was filtered, washed with water, and air dried. The crude product was purified by column chromatography on silica gel using 3:1 methylene chloride:hexane as the eluent. The second band was highly fluorescent and upon evaporation yielded a yellow green solid. Recrystallization from absolute ethanol afforded yellow green needles (1.77 g, 53%), mp 92–93 °C (Table I). Anal. Calcd for C₃₈H₅₀N₂O₂S₃: C, 68.83; H, 7.60; N, 4.23. Found: C, 68.93; H, 7.36; N, 4.00. FTIR (KBr) ν (cm⁻¹) 2925, 2850, 1515, 1320, 1050, 755, 725; EIMS (70 eV) m/z 662 (M⁺, 2), 43 (100).

Procedure E. *N*-[4-(Dimethylamino)phenyl]-2-nitroaniline. To a solution of 1-fluoro-2-nitrobenzene (4 g, 0.028 mol) in THF (25 mL) was added a 5% mol equiv excess of *N,N*-dimethyl-1,4-phenylenediamine (4.045 g, 0.03 mol). The mixture was refluxed for 15 h under a nitrogen atmosphere, cooled, poured into cold water, and stirred for 15 min. The crude product was decolorized and recrystallized from ethanol:water (70:30). A second recrystallization afforded reddish brown crystals (2.91 g, 40%), mp 123.5–125 °C. Anal. Calcd for C₁₄H₁₅N₃O₂: C, 65.37; H, 5.88; N, 16.33. Found: C, 65.87; H, 6.01; N, 16.42. FTIR (KBr) ν (cm⁻¹) 3373 (NH), 2895 (CH₃), 1616 and 1504 (aromatic ring), 1566 and 1348 (NO₂); ¹H NMR (CDCl₃) δ 9.3 (s, 1 H, amine NH), 8.1 (d, 1 H, proton on C₃), 7.4–6.45 (m, 7 H, aromatic CH), 2.9 (s, 6 H, CH₃); ¹³C NMR (CDCl₃) δ 149.1, 145.04, 135.48, 132.04, 127.05, 126.65, 126.37, 116.14, 115.04, 113.12, 40.54; MS, m/z 257 (M⁺, 100).

***N*-[4-(Dimethylamino)phenyl]-1,2-diaminobenzene.** To an oxygen-free ethanol:water mixture (90:10, 60 mL) was added *N*-[4-(dimethylamino)phenyl]-2-nitroaniline (2.00 g, 0.08 mol) and sodium sulfide nonahydrate (6.78 g). The mixture was refluxed for 10 h under an inert atmosphere. The major part of the alcohol was evaporated under reduced pressure, and the residue diluted with oxygen free water (50 mL). The precipitate was collected and washed with oxygen-free water. The crude product was dissolved in oxygen-free ethanol, decolorized, and precipitated with water to yield a white precipitate (1.28 g, 72%), mp 83–88 °C. Anal. Calcd for C₁₄H₁₇N₃: C, 73.98; H, 7.54; N, 18.49. Found: C, 74.20; H, 7.46; N, 18.57. FTIR (KBr) ν (cm⁻¹) 3429 and 3339 (NH₂), 1606, 1518 and 1440 (aromatic ring), 2895 (CH₃); ¹H NMR (CF₃COOD) δ 11 (br s, 3 H, CF₃COOH by exchange with amine protons), 6.9–7.8 (m, 8 H, aromatic CH), 3.5 (s, 6 H, CH₃); MS, m/z 227 (M⁺, 100).

***N*-[4-(Dimethylamino)phenyl]-*N'*-benzoyl-1,2-diaminobenzene.** Into a degassed mixture of *N*-methylpyrrolidone (25 mL) and triethylamine (0.53 g, 0.005 mol) was dissolved *N*-[4-(dimethylamino)phenyl]-1,2-diaminobenzene (1.0 g, 0.004 mol). Benzoyl chloride (0.74 g, 0.005 mol) was added over 15 min at

room temperature. This mixture was stirred for 1 h at room temperature under a nitrogen atmosphere. The mixture was then poured into water containing sodium bicarbonate and filtered to yield the crude product (1.28 g, 89%). Recrystallization from acetone and hexane gave pure lemon yellow crystals, mp 145.5–147 °C. Anal. Calcd for C₂₁H₂₁N₃O: C, 76.11; H, 6.39; N, 12.68. Found: C, 76.49; H, 6.39; N, 12.70. FTIR (KBr) ν (cm⁻¹) 3296 (NH), 2895 (aliphatic CH), 1637 (C=O), 1603, 1525 and 1454 (aromatic ring); ¹H NMR (CDCl₃) δ 8.4 (s, 1 H, amine NH), 8.1–6.7 (m, 14 H, aromatic CH), 5.5 (s, 1 H, amine NH), 2.8 (s, 6 H, CH₃); ¹³C NMR (CDCl₃) δ 165.78 (C=O), 146.67, 136.36, 134.79, 131.65, 130.39 (C), 128.59, 127.10, 125.58, 123.03, 122.68, 121.49, 119.97, 114.54 (CH), 41.45 (CH₃); MS, m/z 331 (M⁺, 35), 182 (100).

1-[4-(Dimethylamino)phenyl]-2-phenylbenzimidazole (6). *N*-[4-(Dimethylamino)phenyl]-*N'*-benzoyl-1,2-diaminobenzene (4.4 g, 0.013 mol) was heated at 160 °C for 8 h under a nitrogen atmosphere. The crude product was scraped out of the flask and recrystallized from an ethanol:water mixture to yield white fibrous crystals of product (2.76 g, 66%), mp 158–159 °C (Table I). Anal. Calcd for C₂₁H₁₉N₃: C, 80.48; H, 6.11; N, 13.41. Found: C, 80.67; H, 6.05; N, 13.38. FTIR (KBr) ν (cm⁻¹) 2895 (CH₃), 1608, 1525 and 1474 (aromatic CH); ¹H NMR (CDCl₃) δ 8–6.7 (m, 13 H, aromatic CH), 2.9 (s, 6 H, CH₃); ¹³C NMR (CDCl₃) δ = 152.59, 150.23, 142.91, 138.03, 130.42, 129.40, 129.16, 128.02, 125.41, 125.08, 122.95, 122.60, 119.63, 112.64, 110.70, 40.41 (CH₃); MS, m/z 313 (M⁺, 100).

Procedure F. 2,5-Bis(*N*-phenylbenzimidazol-2-yl)pyridine (11). Freshly prepared pyridine-2,5-dicarbonyl chloride¹⁵ (1.36 g, 0.007 mol) was added to a solution of *N*-phenyl-1,2-phenylenediamine (2.47 g, 0.013 mol) in degassed *N*-methylpyrrolidone (20 mL). The solution was warmed at 80 °C for 15 h. The dark purple solution was poured onto cracked ice (75 g) and filtered, and the crude wet solid recrystallized from ethanol:water to give a purple crystal (2.1 g, 68%), mp 231–236 °C. The product was dissolved in ethanol (20 mL), decolorized, and reprecipitated with water. An additional recrystallization from ethanol:water afforded a pale yellow microcrystalline solid (1.4 g, 45%), mp 238–240 °C (Table I). Anal. Calcd for C₃₁H₂₁N₅: C, 80.33; H, 4.57; N, 15.11. Found: C, 80.52; H, 4.69; N, 15.06. FTIR (KBr) ν (cm⁻¹) 3054 (aromatic CH), 1595 and 1499 (aromatic ring); ¹H NMR (CDCl₃) 7.9–7.2 (br m, aromatic CH); MS, m/z 462 (M⁺, 100).

Procedure G. *N,N*-Bis(2-[4-(dimethylamino)anilino])terephthalamide. *N*-[4-(Dimethylamino)phenyl]-1,2-diaminobenzene (1.0 g, 0.004 mol) was dissolved in a degassed solution of *N*-methylpyrrolidone (15 mL) and triethylamine (0.445 g, 0.004 mol). To this solution was added terephthaloyl chloride (0.446 g, 0.002 mol) over 15 min at room temperature. This mixture was allowed to stir for 1 h at room temperature under a nitrogen atmosphere. The mixture was poured into water containing sodium bicarbonate and filtered to yield the crude product (1.4 g, 54%). Recrystallization from *N,N*-dimethylformamide and acetone gave golden yellow crystals, mp 256–257 °C (by raising the temperature of the melting point apparatus to 250 °C before inserting the sample). Anal. Calcd for C₃₆H₃₆N₆O₂: C, 73.95; H, 6.21; N, 14.37. Found: C, 73.65; H, 6.29; N, 14.36. FTIR (KBr) ν (cm⁻¹) 3374 and 3259 (NH), 2895 (aliphatic CH), 1645 (C=O), 1603, 1518 and 1446 (aromatic ring); ¹H NMR (CF₃COOD) δ 11.8 (s, 4 H, CF₃COOH by exchange with amine protons), 8.15–7.35 (m, 20 H, aromatic CH), 3.5 (s, 12 H, CH₃); MS, m/z 584 (M⁺, 4), 182 (100).

1,4-Bis(1-[4-(dimethylamino)phenyl]benzimidazol-2-yl)-benzene (12). A solution of *N,N'*-bis(2-[4-(dimethylamino)anilino])terephthalamide (2.0 g, 0.003 mol) in *N*-methylpyrrolidone (5 mL) was heated under nitrogen at 190 °C for 16 h. The mixture was poured into water, filtered, and washed with acetone to yield a white solid (1.37 g, 73%), mp >320 °C (Table I). Anal. Calcd for C₃₆H₃₂N₈: C, 78.81; H, 5.88; N, 15.32. Found: C, 79.15; H, 5.80; N, 15.36. FTIR (KBr) ν (cm⁻¹) 2889 (aliphatic CH), 1606, 1526 and 1454 (aromatic ring); ¹H NMR (CF₃COOD) δ 8.15–7.15 (m, 20 H, aromatic CH), 3.6 (s, 12 H, CH₃); MS, m/z 548 (M⁺, 66), 44 (100).

Registry No. 1, 883-93-2; 2, 716-80-3; 3, 34243-38-4; 4, 59066-61-4; 5, 129922-09-4; 6, 129922-10-7; 7, 904-39-2; 8, 5153-65-1; 9, 18013-43-9; 10, 129922-11-8; 11, 129922-12-9; 12, 129922-13-0.